Observation of $e^+e^- \to \chi_{c1}$ at BESIII

Anja Brueggemann[1,*] on behalf of the BESIII collaboration

[1]Institute of Nuclear Physics, University of Münster, Wilhelm-Klemm-Straße 9, 48149 Münster, Germany

Abstract. In electron-positron annihilations, the process of $e^+e^- \to \chi_{c1}$ can occur via the production of two virtual photons or through neutral current, therefore being suppressed with respect to the normal annihilation process via one virtual photon. Using a dedicated scan sample around the χ_{c1} mass, the direct production of χ_{c1} has been established for the first time in experiments. This provides a new approach for the study of the internal nature of hadrons.

1 Introduction

The dominant process in collisions of electrons and positrons is their electromagnetic annihilation into a single virtual photon, which can immediately decay into a quark-antiquark pair. Due to the restriction to color-neutral states in quantum chromodynamics (QCD) and the conservation of parity P and charge conjugation C in electromagnetic processes, the quark and antiquark must be of the same flavor forming a bound quarkonium state that has the same quantum numbers as the virtual photon with $J^{PC} = 1^{--}$, where J denotes the total angular momentum. In e^+e^- annihilations, vector quarkonia are thus predominantly produced. In the energy region of charmonium quarkonia, which are composed of a charm-anticharm quark pair, the BESIII experiment at the e^+e^- collider BEPCII has collected large data samples at different energies [1], including the world's largest samples of the ground-state vector charmonium J/ψ [2] and its first excitations $\psi(3686)$ [3] and $\psi(3770)$ [4].

The direct production of non-vector states, such as C-even resonances, should also be observable, but is suppressed since the mechanism by a single virtual photon is forbidden. However, it is allowed by higher order electromagnetic processes, i.e. by two or more virtual photons, or by the weak neutral current. Theoretically, the direct production of C-even resonances was suggested for the first time as early as 1978 [5]. At the same time, their experimental observation has so far remained unsuccessful [6–12]. In almost all cases, no candidate events were found [6–10, 12]. In 2020, the SND collaboration observed two candidate events for the directly produced axial vector ($J^{PC} = 1^{++}$) resonance $f_1(1285)$ with a significance of 2.5σ, based on data taken at the e^+e^- collider VEPP-2000 [11].

The strong motivation to search for directly produced non-vector resonances in e^+e^- annihilations is that it provides a new approach to precisely determine the resonances properties, including their mass and total width. At BESIII, one of the most promising candidates to search for is the axial vector charmonium χ_{c1}, which is directly produced either by two virtual photons or by the neutral current, with the first process predicted to dominate [13].

*e-mail: a_drie04@uni-muenster.de

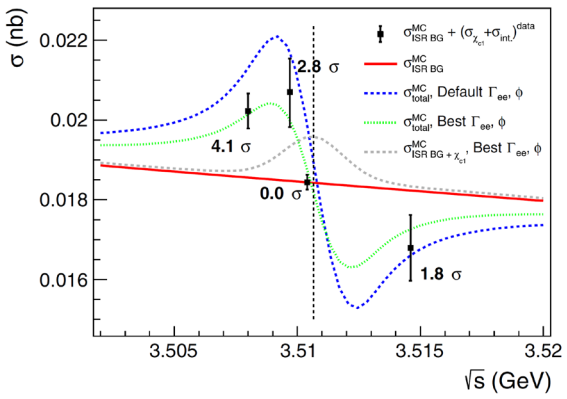

Figure 1. Cross sections for the reaction $e^+e^- \to \gamma J/\psi \to \gamma\mu^+\mu^-$ as function of the center-of-mass energy for different $(\Gamma_{ee}^{\chi_{c1}}, \phi)$ parameter sets. Including $e^+e^- \to \chi_{c1}$ and interference between the direct χ_{c1} production and irreducible ISR background, the blue (green) curve is obtained using the default parameter set from Ref. [18] (the measured set). The gray curve is based on the measured parameter set, where interference is excluded. If only the irreducible ISR background is considered, the red curve results. The χ_{c1} mass is highlighted by the black dashed line. For the four energy points of the χ_{c1} scan data, $\sigma_{\text{ISR BG}}^{\text{MC}} + (\sigma_{\chi_{c1}} + \sigma_{\text{int}})^{\text{data}}$ are shown as black dots with error bars together with the statistical significances of the χ_{c1} production. Figure taken from Ref. [21].

2 Theoretical Predictions and Proposed Analysis Strategy

Since the production amplitude of the process $e^+e^- \to \chi_{c1}$ is unknown but proportional to the χ_{c1} electronic width $\Gamma_{ee}^{\chi_{c1}}$, knowledge of $\Gamma_{ee}^{\chi_{c1}}$ allows access to the cross section. Based on different models, theoretical studies [5, 13–18] already give results for $\Gamma_{ee}^{\chi_{c1}}$ between 0.044 eV [13] and 0.46 eV [5], with the lower limit obtained by calculations requiring unitarity. More recent predictions use the vector meson dominance model [16] or non-relativistic QCD [17] and give $\Gamma_{ee}^{\chi_{c1}} \approx 0.1$ eV.

The latest prediction of 0.41 eV by Ref. [18] additionally provides a comprehensive theoretical framework for an entire analysis to experimentally search for the reaction $e^+e^- \to \chi_{c1}$, taking into account interference between a dedicated signal reaction and background processes. As signal, the process $e^+e^- \to \chi_{c1} \to \gamma J/\psi \to \gamma\mu^+\mu^-$ is considered. It includes the main χ_{c1} decay channel [19] and a final state that is easy to identify. The two relevant background reactions $e^+e^- \to \gamma_{\text{ISR}} J/\psi \to \gamma_{\text{ISR}}\mu^+\mu^-$ and $e^+e^- \to \gamma_{\text{ISR}}\mu^+\mu^-$ show the same final state as the signal process and the emission of an initial state radiation (ISR) photon before the e^+e^- system annihilates via a single virtual photon either into the intermediate resonance J/ψ or directly into to the muon pair. The amplitudes of these two irreducible ISR background processes as well as the signal amplitude along with interference contributions are implemented in the PHOKHARA Monte Carlo (MC) event generator [20].

Based on events simulated by PHOKHARA with $\Gamma_{ee}^{\chi_{c1}} = 0.41$ eV and the relative phase $\phi = 212°$ between signal and background as input parameters [18], the energy-dependent cross section for the direct χ_{c1} production is obtained, which is shown in Fig.1 with the blue dashed line. It exhibits an interference pattern that shows an enhancement below and a reduction of events above the χ_{c1} mass compared to the case where only the background amplitudes are considered, which is represented by the red solid line. Directly at the χ_{c1} mass, almost no signal contribution beyond the background is expected. Given that the signal component is up to 75% above the irreducible ISR background [18], the predicted interference pattern is expected to be measurable with the BESIII detector by an energy scan in the χ_{c1} vicinity. A corresponding study has been performed at BESIII in 2022 [21] using already available data samples.

3 BESIII Detector and Data Samples

The BESIII detector [22] records symmetric e^+e^- collisions provided by the BEPCII storage ring [23] in the center-of-mass (cms) energy range from $\sqrt{s}$ = 2.0 GeV to 4.95 GeV, with a peak luminosity of $1\text{x}10^{33}$ cm^{-2}s^{-1} achieved at $\sqrt{s}$ = 3.77 GeV. The cylindrical core of the BESIII detector covers 93% of the full solid angle and consists of a helium-based multilayer drift chamber (MDC), a plastic scintillator time-of-flight system (TOF), and a CsI(Tl) electromagnetic calorimeter (EMC), which are all enclosed in a superconducting solenoidal magnet providing a 1.0 T magnetic field. The solenoid is supported by an octagonal flux-return yoke with resistive plate counter muon identification modules interleaved with steel. The charged-particle momentum resolution at 1 GeV/c is 0.5%, and the dE/dx resolution is 6% for electrons from Bhabha scattering. The EMC measures photon energies with a resolution of 2.5% (5%) at 1 GeV in the barrel (end cap) region. The time resolution in the TOF barrel region is 68 ps, while that in the end cap region was 110 ps. The end cap TOF system was upgraded in 2015, providing a time resolution of 60 ps [24].

In 2017, the BESIII collaboration collected four data points in the vicinity of the χ_{c1} resonance at $\sqrt{s}$ = 3508.0 GeV, 3509.7 GeV, 3510.4 GeV and 3514.6 GeV with a total integrated luminosity of 445.6 pb^{-1} which is determined using Bhabha scattering events, while the beam energy measurement system is taken to determine the cms energies. As marked with black dots in Fig. 1, two data points lie below, one almost at and the fourth above the χ_{c1} mass.
For background studies, four control data samples are considered at cms energies above the χ_{c1} mass with $\sqrt{s}$ = 3581.5 GeV, 3670.2 GeV, 3773.0 GeV and 4178.4 GeV. The first two data points correspond to the 2018 energy-scan around the $\psi(3686)$ resonance with an integrated luminosity of about 85 pb^{-1} each, which is similar to the luminosities of the χ_{c1} scan data points. The last two control data samples are high luminosity samples of about 3000 pb^{-1} each, where the first corresponds to the $\psi(3770)$ data sample collected in 2010 and 2011, and the second is the sample taken in 2016 for open charm analyses.
To determine selection efficiencies and to describe irreducible background reactions, exclusive simulated data samples of 200 Mio. events at each of the above cms energies are produced with a GEANT4-based [25] MC package, which includes the geometric description of the BESIII detector and the detector response. The simulations model the beam energy spread, ISR in the e^+e^- annihilations and the particle decays with the PHOKHARA generator. At each cms energy the signal reaction, a sample of both irreducible ISR background processes with fixed relative size taking $\Gamma_{ee}^{J/\psi}$ of the J/ψ resonance as input parameter, and a simulation of the interference between the signal and irreducible background using experimentally extracted values for $\Gamma_{ee}^{\chi_{c1}}$ and ϕ (see Sec. 5) are produced.
In addition, two inclusive MC simulations at the high luminosity energy points are studied, where the beam energy spread and ISR production processes are simulated using the KKMC [26] generator, while all particle decays are modeled with EVTGEN [27] using branching fractions either taken from the Particle Data Group [19], when available, or otherwise estimated with LUNDCHARM [28]. They include the production of open charm processes, the ISR production of vector charmonium(-like) states, and the continuum processes incorporated in KKMC. Final state radiation from charged final state particles is incorporated using the PHOTOS package.

4 Event Selection and Background Studies

To reconstruct the final state $\gamma\mu^+\mu^-$ only events with at least one photon and two oppositely charged tracks, that have passed general BESIII selection criteria considering the geometrical

detector properties are selected for further analysis. A kinematic fit with four constraints is applied to the four momenta of the final state particles to conserve energy and momentum between the initial e^+e^- system and the final state. Since multiple photon candidates can occur in a single event, the photon that gives the minimum χ^2_{4C} of the kinematic fit is chosen. To distinguish muon-pair candidates from other charged particle pairs, e.g. from Bhabha scattering, the deposited energy in the EMC needs to be smaller than 0.4 GeV, and polar angles of muons in the MDC between $0.8 < |\cos\theta_\mu| < 0.86$, where the EMC is blind, are excluded. To suppress ISR background processes, polar angles of photon candidates of $|\cos\theta_\gamma| > 0.80$ in the EMC end caps are excluded. $\theta_{\mu,\gamma}$ are defined with respect to the symmetry axis of the MDC.

When studying the two inclusive MC simulations and the corresponding control data samples of high luminosity, a negligible background contribution of the false final state of less than 0.2% is observed. However, irreducible background components remain, which are described using the MC simulations of the irreducible ISR background. The approach is tested by unbinned, two-dimensional maximum likelihood fits of MC simulations to all four control data samples separately, considering the invariant mass distribution $M_{\mu^+\mu^-}$ of the muon pair and the distribution of the polar angle of the muons $|\cos\theta_\mu|$, respectively. The corresponding probability density function (PDF) sums a χ_{c1} signal component and a background contribution. The signal component is described by the signal MC simulation at the lowest cms energy of the χ_{c1} scan data sample, multiplied with two Gaussian distributions to account for the differences in resolution and line-shapes between simulation and data, and between the four control data samples. The background component is described by the irreducible background MC simulation at the corresponding control data point. The MC scaling factors in each fit act as free fit parameters and provide the number of χ_{c1} signal events $N_{\chi_{c1}}$ and the number of irreducible ISR background events $N_{\rm bkg}$. Since the control data samples do not contain a χ_{c1} signal contribution, $N_{\chi_{c1}}$ is expected to be zero in the fits.
However, for all four control data samples, a non-zero χ_{c1} signal contribution is observed with a statistical significance of up to 7.5σ, respectively up to 2.2σ when the significance is normalized to the typical integrated luminosity of 180 pb^{-1} of the χ_{c1} scan data samples.
Thus, a discrepancy between data and the MC description of the irreducible background is observed, mainly resulting from the uncertainty of the input parameter $\Gamma^{J/\psi}_{ee}$ and limits on the simulation of the J/ψ ISR production in PHOKHARA. By applying two-dimensional correction factors extracted from a comparison of the irreducible background MC simulation at the high luminosity $\psi(3770)$ energy point along the binned distributions $M_{\mu^+\mu^-}$ and $|\cos\theta_\mu|$, the MC simulations of the irreducible background are corrected event-by-event at all cms energies.
Repeating the above fit to all four control data samples using the corrected MC simulations, no χ_{c1} signal contribution is observed anymore, $N_{\chi_{c1}}$ is consistent with zero within 1σ. Thus, the MC simulations with applied correction factors precisely describe the remaining background in data and can now be used to search for χ_{c1} signal contributions beyond background in the χ_{c1} scan data samples.

5 Analysis Results

At all four χ_{c1} scan data points, $N_{\chi_{c1}}$ is extracted by applying a similar fit approach as above, with only the interference component between the χ_{c1} signal and the irreducible background added to the PDF. The line shapes for the individual components in the PDF are taken from the corresponding MC simulations at the χ_{c1} scan data points with applied correction factors. The free fit parameters $N_{\chi_{c1}}$ and $N_{\rm bkg}$ constrain the interference component by $N_{\rm int} = a(\Gamma^{\chi_{c1}}_{ee}, \phi) \cdot \sqrt{N_{\chi_{c1}} \cdot N_{\rm bkg}}$ where the factor a is calculated from MC predictions as a

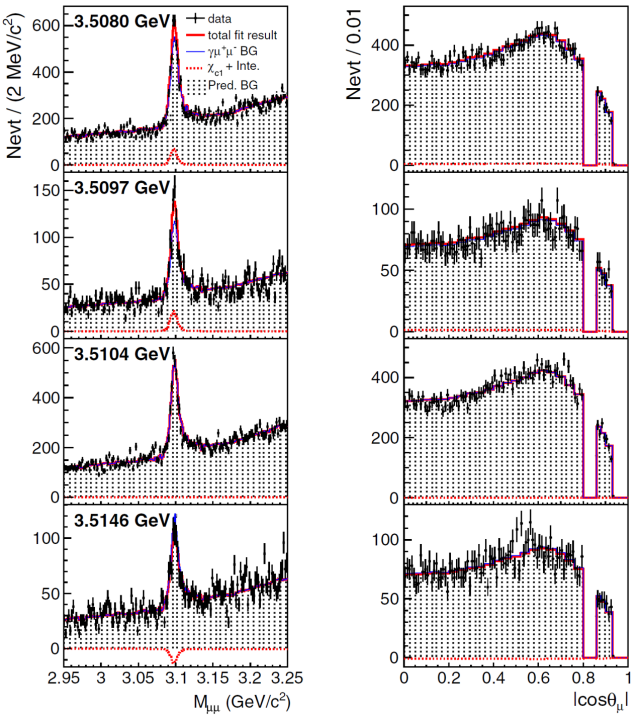

Figure 2. Projections of the two-dimensional fit result onto the invariant mass distribution of the muon pair $M_{\mu^+\mu^-}$ (left) and the distribution of the muons' polar angle $|\cos\theta_\mu|$ (right) at the four χ_{c1} scan energy points. The data are marked as black dots with error bars, the red curve indicates the total fit result, the red dotted and blue dashed curves correspond to the signal component and the irreducible ISR background contribution, respectively. The gray histograms represent the irreducible ISR background component simulated by the PHOKHARA event generator with applied correction factors. Figure taken from Ref. [21].

function of $\Gamma_{ee}^{\chi_{c1}}$ and ϕ, which are extracted from data (details can be found below).
In Fig. 2 the fit results are projected onto the $M_{\mu^+\mu^-}$ and $|\cos\theta_\mu|$ distributions. Signal contributions $N_{\rm sig} = N_{\chi_{c1}} + N_{\rm int}$ are observed beyond the irreducible background. At the cms energies below the χ_{c1} mass, positive signal components of $N_{\rm sig} = 210 \pm 52 \pm 18$ with a statistical significance of (4.1σ) and $N_{\rm sig} = 63 \pm 24 \pm 6$ with (2.8σ) are obtained, the first uncertainty being statistical and the second systematic. Almost at the χ_{c1} mass, no signal contribution is seen with $N_{\rm sig} = 0^{+16}_{-19} \pm 23$ (0.0σ). Above the χ_{c1} mass, a negative signal component with $N_{\rm sig} = -40 \pm 22 \pm 7$ (1.8σ) is observed. Combining the corresponding statistical significances (lowest significances taking systematic effects into account) by summing the logarithms of the maximum likelihoods of the individual fits, 5.3σ (5.1σ) is obtained.
Using the results for $N_{\rm sig}$, the integrated luminosities $\mathcal{L}_{\rm int}$ and the selection efficiencies ϵ determined with the signal MC simulations, the cross-section component extracted from data is determined. Adding the cross-section component of the irreducible ISR background calculated with PHOKHARA, the total cross section $\sigma_{\rm tot} = \sigma^{\rm MC}_{\rm ISR\ BG} + (\sigma_{\chi_{c1}} + \sigma_{\rm int})^{\rm data} = \sigma^{\rm MC}_{\rm ISR\ BG} + N_{\rm int}/(\mathcal{L}\cdot\epsilon)$ is obtained for each χ_{c1} scan data point, as shown in Fig. 1 with the data points marked in black. They follow the general interference pattern as expected in Ref. [18]. However, calculating the line shape of the total cross section for the experimentally measured parameter set of $(\Gamma_{ee}^{\chi_{c1}}, \phi)$ using PHOKHARA provides the green line in Fig. 1, which still shows a discrepancy to the theoretical prediction of the blue line.

In general, Γ_{ee} of a resonance is extracted by fitting the data using an analytical expression of the total cross section, with Γ_{ee} and ϕ as free fit parameters. Here, however, the analytical formula is not straightforward, so a scan method is used to determine Γ_{ee} and ϕ from data.
For this purpose, MC simulations of 200 Mio. events each at all four χ_{c1} scan data points for different parameter sets $(\Gamma_{ee}^{\chi_{c1}}, \phi)$ are generated. A small region of the tested parameter space is shown in Fig. 3 by the black circles. Each parameter set is analyzed by applying the same

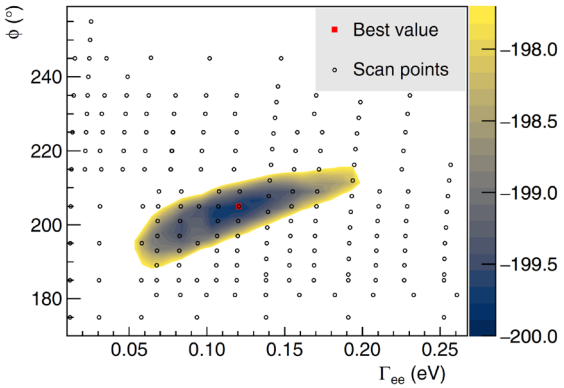

Figure 3. Detailed view of the tested parameter space, where each black circle indicates a single parameter set ($\Gamma_{ee}^{\chi_{c1}}$, ϕ) and the red square corresponds to the set that gives the best fit solution with maximum log-likelihood value. The 68.3% confidence interval of the best parameter set is shown as function of the log-likelihood value. Figure taken from Ref. [21].

fit method as before. The difference is that the four χ_{c1} scan data samples are now fitted simultaneously with the corrected MC simulations, where $N_{\chi_{c1}}$ and N_{bkg} are fixed to the values calculated by MC. The parameter set that yields the maximum likelihood value is shown in Fig. 3 with the red square together with the 68.3% confidence-level region. It provides the best solution of the scan and gives a value of $\Gamma_{ee}^{\chi_{c1}} = (0.12^{+0.08}_{-0.07})$ eV for the χ_{c1} electronic width and $\phi = (205^{+10.0}_{-17.0})^\circ$ for the relative phase, where the uncertainties are statistical. Including the systematic uncertainties, which are in the same order of magnitude as the statistical ones, one obtains $\Gamma_{ee}^{\chi_{c1}} = (0.12^{+0.13}_{-0.08})$ eV and $\phi = (205^{+15.4}_{-22.4})^\circ$. The phase agrees well with the theoretical prediction of 212° [18] and the electronic width is of the same order of magnitude as the theoretical calculations [5, 13–18]. The sources of the systematic uncertainties are the measurements of the cms energies, integrated luminosities, beam energy spread and selection efficiencies, the reconstruction of photon and muon candidates, the constraint on the $|\cos\theta_\gamma|$ distribution, the study of the background components of the false final state, fit ranges and line shapes used, and the extraction of the two-dimensional correction factors. Other sources are found to be negligible.

6 Summary and Outlook

In 2022, the BESIII collaboration at the e^+e^- collider BEPCII published in Ref. [21] the first significant observation of a directly produced non-vector state in e^+e^- annihilations, the axial vector charmonium χ_{c1}, with a significance larger than 5σ. In addition, the first experimental determination of the χ_{c1} electronic width is provided, which is in the same order of magnitude as theoretical calculations [5, 13–18].
Inspired by the analysis strategy proposed in Ref. [18], a new experimental approach to search for directly produced non-vector states in e^+e^- collisions is applied in this study. It is based on an energy scan in the vicinity of the searched resonance and MC simulations to describe signal, background and possible interference between them. Using these simulations, signal contributions beyond background are searched for in the data samples. Furthermore, by applying a scan method, it is shown that the electronic width of the resonance is also experimentally accessible.
For further analyses and verification of the new analysis approach, the tensor ($J^{PC} = 2^{++}$) charmonium χ_{c2} is a promising next candidate for the search for direct production at BESIII, with a complete theoretical framework also presented in Ref. [18].

This work is supported by the German Research Foundation (DFG) under the project number 443159800 and the DFG Research Training Group 2149/2.

References

[1] M. Ablikim *et al.* (BESIII Collaboration), Chin. Phys. C **44**, 040001 (2020)
[2] M. Ablikim *et al.* (BESIII Collaboration), Chin. Phys. C **46**, 074001 (2022)
[3] M. Ablikim *et al.* (BESIII Collaboration), Chin. Phys. C **42**, 023001 (2018)
[4] M. Ablikim *et al.* (BESIII Collaboration), Chin. Phys. C 37, 123001 (2013); Phys. Lett. B **753**, 629 (2016)
[5] J. Kaplan, and J. H. Kühn, Phys. Lett. B **78**, 252 (1978)
[6] P. V. Vorobev *et al.* (ND Collaboration), Sov. J. Nucl. Phys. **48**, 273 (1988)
[7] M. N. Achasov *et al.* (SND Collaboration), Phys. Lett. B **492**, 8 (2000)
[8] M. N. Achasov *et al.* (SND Collaboration), Phys. Rev. D **91**, 092010 (2015)
[9] R. R. Akhmetshin *et al.* (CMD Collaboration), Phys. Lett. B **740**, 273 (2015)
[10] M. N. Achasov *et al.* (SND Collaboration), Phys. Rev. D **98**, 052007 (2018)
[11] M. N. Achasov *et al.* (SND Collaboration), Phys. Lett. B **800**, 135074 (2020)
[12] M. Ablikim *et al.* (BESIII Collaboration), Phys. Rev. D **107**, 032007 (2023)
[13] J. Kaplan, J. H. Kühn, and E. G. O. Safiani, Nucl. Phys. B **157**, 125 (1979)
[14] N. N. Achasov, JETP Lett. **63**, 601 (1996)
[15] D. Yang, and S. Zhao, Eur. Phys. J. C **72**, 1996 (2012)
[16] A. Denig, F. K. Guo, C. Hanhart, and A. V. Nefediev, Phys. Lett. B **736**, 221 (2014)
[17] N. Kivel, and M. Vanderhaeghen, J. High Energy Phys. **02**, 032 (2016)
[18] H. Czyż, J. H. Kühn, and S. Tracz, Phys. Rev. D **94**, 034033 (2016)
[19] R. L. Workman *et al.* (Particle Data Group), Prog. of Theo. and Exp. Phys. **2022**, 083C01 (2022)
[20] H. Czyż, A. Grzelińska, and J. H. Kühn, Phys. Rev. D **81**, 094014 (2010)
[21] M. Ablikim *et al.* (BESIII Collaboration), "First Observation of the Direct Production of the χ_{c1} in e^+e^- Annihilation", Phys. Rev. Lett. **129**, 122001 (2022), DOI: 10.1103/PhysRevLett.129.122001
[22] M. Ablikim *et al.* (BESIII Collaboration), Nucl. Instrum. Meth. A **614**, 345 (2010)
[23] C. H. Yu *et al.*, Proc. 7th Int. Particle Accelerator Conf. (IPAC'16), Busan, Korea, 1014 (2016)
[24] X. Li *et al.*, Radiat. Detect. Technol. Methods **1**, 13 (2017); Y. X. Guo *et al.*, Radiat. Detect. Technol. Methods **1**, 15 (2017); P. Cao *et al.*, Nucl. Instrum. Meth. A **953**, 163053 (2020)
[25] S. Agostinelli *et al.* (GEANT4 Collaboration), Nucl. Instrum. Meth. A **506**, 250 (2003)
[26] S. Jadach, B. F. L. Ward and Z. Was, Phys. Rev. D **63**, 113009 (2001); Comput. Phys. Commun. 130, 260 (2000)
[27] D. J. Lange, Nucl. Instrum. Meth. A **462**, 152 (2001); R. G. Ping, Chin. Phys. C **32**, 599 (2008)
[28] J. C. Chen, G. S. Huang, X. R. Qi, D. H. Zhang, and Y. S. Zhu, Phys. Rev. D **62**, 034003 (2000); R. L. Yang, R. G. Ping, and H. Chen, Chin. Phys. Lett. **31**, 061301 (2014)
[29] E. Barberio, B. van Eijk, and Z. Was, Comput. Phys. Commun. **66**, 115 (1991)